

<sup>5</sup>Carole Jordan, Mon. Not. R. Astron. Soc. **142**, 501 (1969).

<sup>6</sup>G. Lüders, Ann. Phys. (Paris) **8**, 301 (1951).

<sup>7</sup>From Ref. 3 it can be inferred that collisional mixing does not take place before radiative deactivation at the densities considered here.

## Position and Dynamics of Ag Ions in Superionic AgI Using Extended X-Ray Absorption Fine Structure\*

J. B. Boyce, T. M. Hayes, W. Stutius, and J. C. Mikkelsen, Jr.

*Xerox Palo Alto Research Center, Palo Alto, California 94304*

(Received 3 February 1977)

By use of extended x-ray absorption fine structure, the Ag ions in superionic AgI are shown to occupy the distorted tetrahedral sites in the iodine bcc lattice, being slightly displaced from the center toward the faces along the most probable diffusion path. The residence time of the Ag ions in these sites is determined to be longer than their flight time, implying that the jump-diffusion model is more appropriate than a free-diffusion model.

AgI is typical of a class of superionic conductors that achieve their high-conducting state through a structural phase transition. Below 147°C, AgI has the hexagonal wurtzite structure ( $\beta$  phase). At 147°C, it transforms to the  $\alpha$  phase in which the iodine ions form a body-centered cubic lattice with the Ag sublattice disordered,<sup>1,2</sup> and the ionic conductivity increases by 4 orders of magnitude to  $1 (\Omega \text{ cm})^{-1}$ .<sup>3</sup> We have used the extended x-ray absorption fine structure (EXAFS) on the Ag *K*-shell absorption to obtain information on both the position and the dynamics of the Ag ions in the superionic  $\alpha$  phase of AgI. First, we show that the Ag-ion position distribution function is peaked  $\sim 0.1 \text{ \AA}$  from the center of the distorted tetrahedron formed by the bcc iodine lattice, displaced toward a tetrahedral face. Secondly, we determine that the residence time of the Ag ions in the displaced tetrahedral site is roughly 3 times the flight time between different tetrahedra. Finally, we show that previous conclusions on the position and dynamics of the Ag ions in superionic AgI which were drawn from x-ray<sup>1,2</sup> and neutron<sup>4,5</sup> scattering studies are inconsistent with the EXAFS data.

The EXAFS on the Ag *K*-shell absorption in AgI was measured in the ionic insulating  $\beta$  phase at 20°C and 98°C and in the superionic  $\alpha$  phase at 198°C and 302°C using the facilities of the Stanford Linear Accelerator Center Synchrotron Radiation Project. The EXAFS is observed as an oscillation in the absorption cross section above the Ag *K* edge.<sup>6</sup> Using procedures which have been described in detail elsewhere,<sup>7</sup> we extracted the EXAFS as a function of final-state electron

momentum,  $k$ , from the measured absorption and made a Fourier transformation into real space. The resultant complex transform,  $\varphi(r)$ , is shown in Fig. 1 for the 20°C and the 198°C data. Note that the vertical scales differ by a factor of 2. All the data were collected on the same sample and were reduced in an identical manner.

The Fourier transform,  $\varphi(r)$ , of the EXAFS on *K*-shell absorption can be expressed<sup>7</sup> as a sum of contributions,  $\xi$ , from each shell of atoms surrounding the excited atom:

$$\varphi(r) = \sum_{\alpha} \int_0^{\infty} (dr'/r'^2) p_{\alpha}(r') \xi_{\alpha}(r-r'), \quad (1)$$

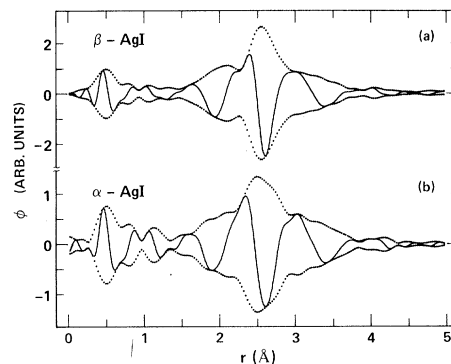


FIG. 1. The real part (solid line) and the magnitude of the Fourier transform  $\varphi(r)$  of the EXAFS on the Ag *K*-shell absorption in AgI: (a) at 20°C (well below the normal-superionic transition) and (b) at 198°C (well above the transition). Note that the vertical scales differ by a factor of 2. The data were collected on the same sample and transformed over the same interval in  $k$  space.

where  $r > 0$  and  $p_\alpha$  is the radial distribution function of the  $\alpha$ th atomic species. As in x-ray and neutron diffraction studies,  $\varphi$  is a radial distribution function modified by convolution with a peak function,  $\xi$ .  $\xi(r)$  is a complicated function involving the complex  $t$  matrix of the scattering atom, the final-state electron lifetime, and the initial phase shift due to the excited-atom potential. In addition,  $\xi$  is a function of the manner in which the finite range of the  $k$ -space data is treated. In order to enable direct comparison among the data at different temperatures, we have used in each case the same square window,  $k = 3$  to  $17 \text{ \AA}^{-1}$ , Gaussian broadened with  $\sigma_w = 0.7 \text{ \AA}^{-1}$ .  $\xi$  is insensitive, however, to changes in crystal structure, local bonding, thermal effects, etc. The strategy of our study, therefore, is to extract  $\xi(r)$  from the  $\varphi$  measured in a state where  $p(r)$  is known, at  $20^\circ\text{C}$  in the  $\beta$  phase. The unknown  $p(r)$  at other temperatures can then be obtained from the appropriate  $\varphi$  using this  $\xi$ .<sup>7</sup>

Before discussing the change of the EXAFS of AgI with temperature, we first consider the  $20^\circ\text{C}$  data. At this temperature AgI has the hexagonal wurtzite structure in which each Ag atom has four iodine nearest neighbors at  $2.82 \text{ \AA}$  and twelve Ag next-nearest neighbors at  $4.59 \text{ \AA}$ . The structure below  $1.5 \text{ \AA}$  in both Figs. 1(a) and 1(b) is an artifact of the data-reduction techniques. The absence of any significant structure beyond  $3.8 \text{ \AA}$  in Fig. 1(a) suggests that only the nearest-neighbor iodine atoms contribute substantially to the EXAFS. They give rise to the extensive structure between  $1.6$  and  $3.8 \text{ \AA}$  which peaks at  $1.56 \text{ \AA}$ ,  $0.26 \text{ \AA}$  below the actual peak in the radial distribution due to the  $k$  dependence of the initial phase shift and of the phase of the  $t$  matrix. The general shape in real space, including the satellite at  $2.1 \text{ \AA}$  and the shoulder at  $3.1 \text{ \AA}$ , is reproduced in each of our measurements on AgI. In fact, the only significant difference between the data in the ionic insulating phase at  $20^\circ\text{C}$  and  $98^\circ\text{C}$  is that the peak in the higher-temperature data is broadened somewhat and reduced in intensity by about 10%. In analogy with x-ray and neutron scattering we define the reliability index by

$$R = \frac{\sum (|\text{Re}(\varphi_0 - \varphi_M)| + |\text{Im}(\varphi_0 - \varphi_M)|)}{\sum (|\text{Re}\varphi_0| + |\text{Im}\varphi_0|)},$$

where  $\varphi_0$  is the experimentally determined EXAFS real-space function,  $\varphi_M$  is the model function simulated from the  $20^\circ\text{C}$  data, and the sum is over all the data points in the interval  $r = 1.6$ – $3.8 \text{ \AA}$ . These  $98^\circ\text{C}$  data can be fitted by Gaussian

broadening the  $20^\circ\text{C}$  data by  $0.05 \text{ \AA}$  with a reliability index of  $R = 0.06$ . This  $R$  places an upper bound on the accumulated errors from the original data and from the data-reduction process.

Having obtained a  $\xi_I$  for iodine scatterers and a measure of the expected  $R$  value for a good fit using the  $\beta$ -phase data, we now turn to examine the  $\varphi$  for AgI in the superionic  $\alpha$  phase. It is evident that two different types of changes occur between Figs. 1(a) and 1(b). First, the main peak shifts to lower  $r$  and develops a shoulder at higher  $r$ . Secondly, the height of the peak decreases. Consider first the positional information contained in the peak shifts. We assume that, as in the  $\beta$  phase, there are no Ag-Ag nearest neighbors and synthesize the  $198^\circ\text{C}$  peak using the  $\xi_I$  extracted at  $20^\circ\text{C}$ . We initially attempted to fit the data using a single Gaussian-broadened peak. This fit required a slight shift to lower Ag-I spacing than at  $20^\circ\text{C}$  ( $r = 2.81 \text{ \AA}$  instead of  $r = 2.82 \text{ \AA}$ ), an additional Gaussian broadening of  $0.07 \text{ \AA}$ , and a further amplitude reduction of 22%, and yielded  $R = 0.12$ . An  $R$  value of 0.12 is too large to be satisfactory, even taking into account the reduction of signal between  $98$  and  $198^\circ\text{C}$ . Furthermore, the deviation between  $\varphi_M$  and  $\varphi_0$  is systematic and suggests that a bimodal radial distribution is more appropriate. It is clear even from this first fit, however, that the nearest neighbors of Ag are I ions at a position corresponding roughly to the center of the tetrahedral sites ( $r = 2.82 \text{ \AA}$  from the known<sup>2</sup> x-ray lattice constant at  $200^\circ\text{C}$  of  $5.05 \text{ \AA}$ ). The  $198^\circ\text{C}$  data are inconsistent with any significant number of Ag ions being near the center of the trigonal site ( $r = 2.68 \text{ \AA}$ ). This conclusion of tetrahedral symmetry for the Ag ions is consistent with the similarity between the Raman spectra<sup>8</sup> in the  $\beta$  and  $\alpha$  phases. Accordingly, we will restrict our search to models which are appropriate to the tetrahedral sites but displaced somewhat to yield the bimodal distribution suggested by the EXAFS data.

Let us consider the following two models: (a) a displacement of Ag along the (100) direction with two I ions closer and two farther than  $2.82 \text{ \AA}$ ; (b) a displacement of Ag along the (110) direction with three I atoms closer and one farther than  $2.82 \text{ \AA}$ . The latter model is most attractive as it calls for the Ag being displaced toward a tetrahedral face along a likely path for diffusion among tetrahedra, whereas the first model displaces the Ag ions toward the small space between adjacent I ions. A fit by model (a) requires two atoms at  $2.75 \text{ \AA}$  and two at  $2.87 \text{ \AA}$  and a further amplitude

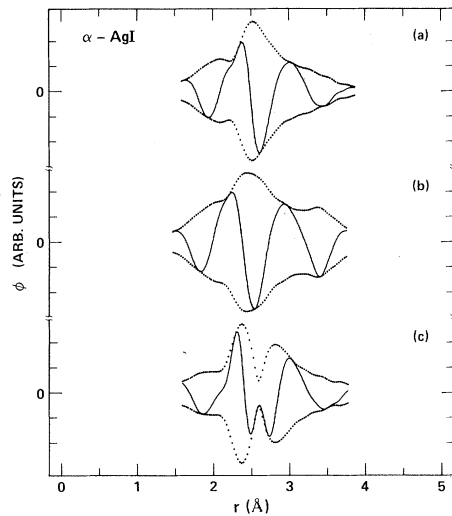


FIG. 2. Synthesis of the Fourier transform,  $\phi(r)$ , from Fig. 1(b) for the superionic phase at 198°C, using three different structural models: (a) Ag in displaced tetrahedral sites with three iodine at  $r=2.78$  Å and one iodine at  $r=2.93$  Å; (b) Stroock model (Refs. 1 and 2) from x-ray scattering; (c) Bührer-Hälg model (Ref. 4) from neutron scattering. (b) and (c) do not reproduce the measured EXAFS, whereas (a) does.

reduction of 25%, yielding  $R=0.11$ . This is not satisfactory because the  $R$  value is still large, the radii are slightly too small, and systematic deviations between  $\phi_0$  and  $\phi_M$  still remain. Finally, model (b) requires three I atoms at 2.78 Å and one at 2.93 Å and a further amplitude reduction of 25%, yielding  $R=0.09$ . In this case, illustrated in Fig. 2(a), the  $R$  value is significantly lower, the radii are appropriate (giving  $r=2.82$  Å for the center of the tetrahedron), and the systematic deviations between  $\phi_0$  and  $\phi_M$  have been eliminated. We can conclude, accordingly, that at 198°C the Ag are in the vicinity of the tetrahedral sites and have lost  $\sim 25\%$  of their EXAFS amplitude compared with the 20°C data.<sup>9</sup> Additionally, the above evidence favors model (b), where the Ag ions are displaced by  $\sim 0.1$  Å from the center of the tetrahedron along the (110) direction toward a tetrahedral face. Within a given model the change in  $R$  value suggests the following error limits: amplitude,  $\pm 5\%$ ; position,  $\pm 0.01$  Å. The data in the superionic phase at the higher temperature of 302°C are fitted in the same manner but with an additional broadening of 0.04 Å.

It is interesting to note that the two peaks with which we synthesize the  $\phi$  at 198 and 302°C are nearly as narrow as the first-neighbor peak in

the  $\phi$  at 20°C, which we estimate to have a Gaussian half-width less than 0.1 Å. The broadening in the nearest-neighbor position which is observed in EXAFS should not be confused with the much larger rms deviation from the average lattice position deduced from x-ray and neutron diffraction studies ( $\approx 0.5$  Å for I and 0.7 Å for Ag at 195°C).<sup>4</sup> The latter broadening includes effects which do not broaden the EXAFS, such as long-wavelength acoustic phonons and certain types of static disorder.

In the same manner we have also synthesized the EXAFS that one *would expect* from the two other structural models which have been proposed. These are shown in Figs. 2(b) and 2(c). Figure 2(b) corresponds to the Stroock model,<sup>1,2</sup> where two Ag ions are equally distributed over 42 crystallographic sites in the cube formed by the bcc iodine atoms. The  $R$  value for this model is 0.60, the poor agreement due mainly to the large number of neighbors in the trigonal sites at  $r=2.68$  Å. Figure 2(c) results from the model proposed by Bührer and Hälg<sup>4</sup> from neutron scattering experiments, in which the Ag ions occupy the displaced tetrahedral 24g sites having two iodine near neighbors at  $r=2.71$  Å and the other two at  $r=2.96$  Å.  $R$  equals 0.50 for this structural model, the sizable deviation due mainly to the large displacement from the tetrahedral center. It is seen that both of these two structural models are, therefore, inconsistent with the EXAFS data and so must be ruled out.

Next, we consider the information contained in the amplitude of the EXAFS peaks in real space. In the synthesis of the 198°C data, it was necessary to reduce the amplitude of the peaks by  $\sim 25\%$  in order to obtain the experimental amplitude. This implies that only  $\sim 75\%$  of the Ag atoms that were observed at room temperature are contributing to the sharp EXAFS features at high temperature. Such a loss in intensity can be explained by considering the following simple model. An Ag ion resides inside a tetrahedron at one of the displaced sites for a residence time  $\tau_R$  and during this time yields a sharp EXAFS signal. During the flight time,  $\tau_F$ , between adjacent tetrahedra the Ag-I distances are distributed over a large range and so will not contribute to  $\phi$ . Accordingly, the total intensity of the sharp features equals  $\tau_R/(\tau_R+\tau_F)$ , which then is approximately equal to 0.75, yielding  $\tau_R/\tau_F=3.0\pm 0.6$ . Thus  $\tau_R$  is longer than  $\tau_F$ , implying that conduction in the superionic phase of AgI is more closely related to jump diffusion than to free diffusion.<sup>10</sup>

An estimate of these times can be made since the sum  $\tau_R + \tau_F$  is just the time that enters the jump-diffusion expression for the ionic conductivity,  $\sigma$ :  $\tau_R + \tau_F \approx Ne^2d^2/6k_B T\sigma$ , where  $N$  is the concentration of Ag ions,  $e$  their charge, and  $d$  the mean jump distance. We consider hops between the neighboring tetrahedral sites for which  $d = 1.8$  Å. At 198°C, using  $\sigma = 1.6$  ( $\Omega$  cm)<sup>-1</sup>, we then have  $\tau_R + \tau_F \approx 2.1$  ps.  $\tau_F$  can be estimated using the equipartition theorem and assuming that the potential energy is small during the ion flight:  $\tau_F \approx (Md^2/3k_B T)^{1/2}$ , where  $M$  is the Ag-ion mass. At 198°C this yields  $\tau_F \approx 0.6$  ps, and, therefore,  $\tau_R/\tau_F \approx 2.5$ , in good agreement with the observed value of  $3.9 \pm 0.6$ . This ratio is at variance with the results of an analysis of quasielastic neutron scattering data by Eckold *et al.*,<sup>5</sup> who conclude that the residence time is *shorter* than the flight time ( $\tau_R/\tau_F \approx 0.5$ ). Their results would predict, however, a first-neighbor peak amplitude in the superionic phase which is less than one-half of what we observe.

In summary, we have shown that the Ag ions in the superionic phase of AgI occupy sites slightly displaced from the center of the distorted iodine tetrahedron, yielding sharp EXAFS features with three near-neighbor iodine atoms at  $2.78 \pm 0.01$  Å and one at  $2.93 \pm 0.01$  Å. Secondly, we have determined that the residence time of the Ag ions is longer than their flight time by a factor of 3, sup-

porting the validity of a jump-diffusion model for the conduction.

\*Work partially supported by National Science Foundation Grant No. DMR 73-07692, in cooperation with the Stanford Linear Accelerator Center and the U. S. Energy Research and Development Administration.

<sup>1</sup>L. W. Strock, Z. Phys. Chem., Abt. B 25, 411 (1934), and 31, 132 (1936).

<sup>2</sup>S. Hoshino, J. Phys. Soc. Jpn. 12, 315 (1957).

<sup>3</sup>W. Biermann and W. Jost, Z. Phys. Chem. (Frankfurt am Main) 17, 139 (1960).

<sup>4</sup>W. Bührer and W. Hälgl, Helv. Phys. Acta 47, 27 (1974).

<sup>5</sup>G. Eckold, K. Funke, J. Kalus, and R. E. Lechner, J. Phys. Chem. Solids 37, 1097 (1976).

<sup>6</sup>EXAFS has been discussed at length in the literature. See, for example, F. W. Lytle, D. E. Sayers, and E. A. Stern, Phys. Rev. B 11, 4825 (1975); and E. A. Stern, D. E. Sayers, and F. W. Lytle, Phys. Rev. B 11, 4836 (1975).

<sup>7</sup>T. M. Hayes, P. N. Sen, and S. H. Hunter, J. Phys. C 9, 4357 (1976).

<sup>8</sup>G. Burns, F. H. Dacol, and M. W. Shafer, Solid State Commun. 19, 291 (1976); M. J. Delaney and S. Ushioda, Solid State Commun. 19, 297 (1976).

<sup>9</sup>In a preliminary analysis of their EXAFS data on  $\alpha$ -AgI, D. E. Sayers and E. A. Stern have also observed a reduction (private communication).

<sup>10</sup>B. A. Huberman and P. N. Sen, Phys. Rev. Lett. 33, 1379 (1974).

## Electrodynamics at Metal Boundaries with Inclusion of Plasma Waves

F. Forstmann and H. Stenschke

*Institut für Theoretische Physik, Freie Universität Berlin, 1 Berlin 33, West Germany*

(Received 21 March 1977)

The energy theorem of electrodynamics is cast in a form which yields expressions for the energy current and energy dissipation of a combined field of transverse and longitudinal waves when the longitudinal field is described in the hydrodynamic approximation. This has consequences concerning the boundary conditions for transverse and plasma waves at metal-metal interface and the photoemission yield.

Plasma waves in metals are homogeneous solutions of Maxwell's equations. They are excited by interaction of light with conducting media<sup>1</sup> and therefore should be properly included in optics at metal surfaces. There have been a few attempts to achieve this on a macroscopic level,<sup>2,3</sup> while other authors approached this problem by microscopic models.<sup>4-7</sup>

A macroscopic treatment of plasma waves is most often done via the so-called hydrodynamic approximation of the equation of motion of the

electron gas<sup>8</sup> such that

$$\frac{\partial \vec{j}}{\partial t} = \frac{\omega_p^2}{4\pi} \vec{E} - \gamma \vec{j} - D \nabla \rho, \quad (1)$$

with  $\vec{j}$  and  $\rho$  the current and charge densities,  $\omega_p^2 = 4\pi n e^2/m$ , and  $\gamma = \tau^{-1}$  an inverse lifetime. Equation (1) can be derived from Boltzmann's equation; it contains Ohm's law, the propagation of plasma waves with the dispersion  $\omega(\omega + i\gamma) = \omega_p^2 + DK^2$  (where  $D = \frac{3}{5} v_F^2$  in a free-electron approximation), and a difference in the transverse